Contribution from the Departments of Chemistry, University of Manchester, Manchester M13 9PL, U.K.,
and University of Arizona, Tucson, Arizona 85721

Synthesis of (1,2-Benzenediolato(2-)-*O,O'*)oxobis(1-piperidinolato(1-)-*O,N*)molybdenum(VI), [MoO(C$_5$H$_{10}$NO)$_2$(C$_6$H$_4$O$_2$)], and Structure Determination by Correlated ^{1}H–^{13}C Two-Dimensional NMR Spectroscopy and X-ray Crystallography

STUART BRISTOW,[1a] JOHN H. ENEMARK,*[1b] C. DAVID GARNER,*[1a] MARTIN MINELLI,[1b]
GARETH A. MORRIS,[1a] and RICHARD B. ORTEGA[1b]

cis-[MoO$_2$(C$_5$H$_{10}$NO)$_2$] reacts with 1,2-dihydroxybenzene (H$_2$cat) and its substituted derivatives (4-methyl-, 4-*tert*-butyl-, 4-nitro-, 3,5-di-*tert*-butyl-, and 3,4,5,6-tetrabromocatechol) to form the corresponding [MoO(C$_5$H$_{10}$NO)$_2$(catecholate)] compounds. The structure of [MoO(C$_5$H$_{10}$NO)$_2$(cat)] in solution has been investigated by ^{1}H and ^{13}C NMR spectroscopy, including the use of "two-dimensional" magnetic resonance techniques to determine ^{1}H–^{13}C chemical shift correlations and ^{1}H–^{1}H scalar coupling correlations. The NMR results imply that the molecule has C_s symmetry, with the catecholate ligand lying in the mirror plane. This has been confirmed by an X-ray crystal structure determination. [MoO(C$_5$H$_{10}$NO)$_2$(cat)] crystallizes in the tetragonal space group $P\bar{4}2_1c$, with $a = b = 14.080$ (4) Å, $c = 18.099$ (8) Å, and $Z = 8$. The molecular unit involves a distorted pentagonal-bipyramidal arrangement of O- and N-ligand donor atoms about the molybdenum, with the oxo group (Mo–O$_t$ = 1.688 (6) Å) occupying an axial position and the catecholate(2–) ligand spanning an equatorial and an axial site. A notable aspect of the molecular structure is that there is no appreciable static trans effect due to Mo–O$_t$; thus, the lengths of the Mo–O bonds involving the catecholate(2–) ligand are 2.016 (5) and 2.012 (5) Å, respectively, cis and trans to the oxo group. [MoO(C$_5$H$_{10}$NO)$_2$-(catecholate)] complexes undergo an irreversible one-electron reduction, but at slow cyclic voltammetric scan rates, this approaches a two-electron reduction, as is clearly manifest during controlled-potential electrolysis. The 4-*tert*-butyl- and 3,5-di-*tert*-butyl-catecholate complexes undergo an essentially reversible one-electron oxidation. The potentials at which these redox processes occur vary in the expected manner with the nature of the substitution of the catecholate ring. Details of the UV–vis, IR, and mass spectra recorded for a selection of these complexes are presented.

Introduction

The complexes *cis*-[MoY$_2$(R$_2$NO)$_2$] (Y = O and/or S)$^{2-5}$ constitute an interesting homologous series. We have been interested in the development of the chemistry of these systems^{6,7} and have found that *cis*-[MoO$_2$(C$_5$H$_{10}$NO)$_2$] reacts with several 1,2-dihydroxybenzene derivatives to give compounds of formula [MoO(R$_2$NO)$_2$(catecholate)]. Herein, we present information obtained from structural, spectroscopic, and electrochemical investigations, which establishes the nature and salient properties of this novel class of molybdenum(VI) complexes.

Experimental Section

Analyses and Instrumentation. Microanalyses were carried out by the University of Manchester Microanalytical Laboratory. IR spectra were recorded, for Nujol mulls of the samples held between CsI plates, in the range 4000–200 cm^{-1}, on a Perkin-Elmer 577 grating spectrometer. UV–vis spectra were recorded for solutions of the samples dissolved in CHCl$_3$ on a Perkin-Elmer 402 spectrometer in matched, 0.1 cm path length, silica cells. Mass spectra were obtained for samples sublimed at ca. 200 °C, by using 70 eV electron ionization with an AEI MS-30 instrument. Electrochemical measurements were performed with instrumentation as previously reported.^{7}

NMR spectra were recorded for ca. 0.5 M solutions of the samples in CDCl$_3$. ^{1}H NMR spectra at 300 MHz, carbon-13 NMR spectra at 75 MHz, and two-dimensional ^{1}H–^{13}C and ^{1}H–^{1}H NMR spectra were obtained on a Varian XL-300 spectrometer by the pulse Fourier transform technique, using Me$_4$Si as internal reference. ^{1}H NMR spectra were recorded for samples in 5 mm diameter tubes, rotated at ca. 15 Hz at a temperature of ca. 293 K. ^{13}C NMR spectra (including the two-dimensional spectra) were recorded for samples in 10 mm diameter tubes, rotated at ca. 10 Hz at a temperature of ca. 293 K. The 16.3-MHz ^{95}Mo NMR spectra were recorded on a Bruker WM-250 spectrometer by the

pulse Fourier transform technique, using 2 M Na$_2$MoO$_4$ in D$_2$O at pH 11 as external reference, in 10 mm diameter tubes, which were rotated at ca. 20 Hz; the temperature was ca. 298 K.

Syntheses. All of the compounds reported herein were prepared analytically pure in the manner described for the title complex.

Solid 1,2-dihydroxybenzene (catechol) (0.44 g, 4.0 mmol) was added to a solution of *cis*-[MoO$_2$(C$_5$H$_{10}$NO)$_2$]^3 (1.31 g, 4.0 mmol) in CH$_2$Cl$_2$ (25 cm^3). The mixture was stirred for ca. 1 h, by which time the solution had acquired a deep violet color. This solution was filtered free of a trace amount of a dark solid, and the solvent was removed by evaporation under reduced pressure, yielding a dark violet solid. This crude product was freed of an EPR-active impurity by column chromatography on silica gel (0.2–0.5-mm mesh) using ethyl acetate as eluant. Anal. Calcd for C$_{16}$H$_{24}$N$_2$O$_5$Mo: C, 45.7; H, 5.8; N, 6.7; Mo, 22.8. Found: C, 45.6; H, 5.8; N, 6.7; Mo, 22.8.

This procedure proved suitable for the preparation of analytically pure samples of the corresponding [MoO(C$_5$H$_{10}$NO)$_2$(catecholate)] complexes, for H$_2$catecholate = 4-methylcatechol, 4-*tert*-butylcatechol, 3,5-di-*tert*-butylcatechol, 4-nitrocatechol, or 3,4,5,6-tetrabromocatechol. However, this preparative route has not permitted the isolation of pure samples of the corresponding complexes containing the doubly deprotonated form of 2-aminohydroxybenzene (*o*-aminophenol) or benzene-1,2-dithiol.

Crystal Structure Determination. Rectangular prismatic crystals of [MoO(C$_5$H$_{10}$NO)$_2$(cat)] were obtained by dissolving the compound in boiling methylcyclohexane and slowly cooling the solution. Axial photos showed these crystals to belong to the Laue class 4/*mmm* with $a = b = 9.957$ Å and $c = 18.103$ Å. The data revealed systematic absences 00*l*, *l* = 2*n* + 1, and *h*00, *h* = 2*n* + 1. Pseudosymmetric absences, 0*kl*, *l* = 2*n* + 1, and *hk*0, *h* + *k* = 2*n* + 1, were also observed. General reflections, *hkl*, *l* = 2*n* + 1, were observed to be systematically weak. The most likely space group $P4_2$2$_1$2 coupled with $Z = 4$ led to the proposed molecular structure possessing a two-fold axis. Several attempts to solve the structure in this space group were unsuccessful, as were attempts to solve the structure in $P4_2$, a subgroup of $P4_2$2$_1$2. Other crystals of this batch yielded the same diffraction pattern. It was concluded that the crystals were probably twinned, and another solvent system was sought for the growth of single crystals. After extensive trials, crystals were obtained by diffusing *n*-heptane into a solution of [MoO(C$_5$H$_{10}$NO)$_2$(cat)] in bromoform. These crystals proved suitable for a complete X-ray crystallographic determination, the details of which are summarized in Table V. A dark purple, plate-shaped crystal was mounted on a glass fiber with its long axis roughly parallel to the ϕ axis of the goniometer. Preliminary examination of the crystal and the data collection were accomplished on a Syntex (Nicolet) P2$_1$ diffractometer. The diffractometer software has been modified to include a profile-analyzed prescan, which determines

(1) (a) University of Manchester. (b) University of Arizona.
(2) Hofer, E.; Holzbach, W.; Wieghardt, K. *Angew. Chem., Int. Ed. Engl.* **1981**, *20*, 282.
(3) Wieghardt, K.; Hahn, M.; Weiss, J.; Swiridoff, W. *Z. Anorg. Allg. Chem.* **1982**, *492*, 164.
(4) Gheller, S. R.; Hambley, T. W.; Brownlee, R. T. C.; O'Connor, M. J.; Snow, M. R.; Wedd, A. G. *Aust. J. Chem.* **1982**, *35*, 2183.
(5) Bristow, S.; Collison, D.; Garner, C. D.; Clegg, W. *J. Chem. Soc., Dalton Trans.* **1983**, 2495.
(6) Bristow, S.; Garner, C. D.; Clegg, W. *Inorg. Chim. Acta* **1983**, *76*, L261.
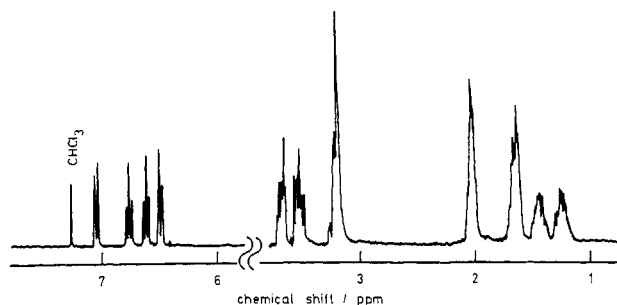(7) Bristow, S.; Garner, C. D.; Pickett, C. J. *J. Chem. Soc., Dalton Trans.* **1984**, 1617.

Figure 1. 300-MHz ^{1}H NMR spectrum of [MoO(C$_5$H$_{10}$NO)$_2$(cat)] in CDCl$_3$.

Figure 2. 75-MHz ^{13}C NMR spectrum of [MoO(C$_5$H$_{10}$NO)$_2$(cat)] in CDCl$_3$.

an optimum scan speed for each reflection so that all reflections have the same $\sigma(F)$ value.

Cell constants and an orientation matrix for data collection were obtained from least-squares refinement, using the setting angles of 23 reflections in the range $5° < 2\theta < 24°$. The cell parameters and calculated volume (Table V) are based on a constrained refinement for a tetragonal cell. Axial photos showed a cell with twice the volume of the previous cell, indicating $Z = 8$. As a check on crystal quality, ω scans of several intense reflections were measured; the width at half-height was 0.25°, indicating good crystal quality. From the systematic absences of hhl, $l = 2n + 1$, and $h00$, $h = 2n + 1$, and from subsequent least-squares refinement, the space group was determined to be $P\bar{4}2_1c$ (No 114). The details of data collection are summarized in Table V. Fixed background counts were made by counting at the extremes of the scan, such that the ratio of peak counting time to background counting time was 2:1. The diameter of the incident-beam collimator was 0.5 mm. As a check on crystal and electronic stability, 2 representative reflections were measured every 98 reflections. The intensities of these standards remained constant within experimental error throughout data collection. No decay or extinction corrections were required.

Details concerning the solution and refinement of the structure are given in Table V. The standard deviation of a corrected intensity $\sigma(F_o^2)$ is defined by

$$\sigma^2(F_o^2) = \sigma^2(I) + (pI)^2$$

where $\sigma(I)$ is the standard deviation of the intensity based on counting statistics and p is a factor introduced to downweight intense reflections. Here p was set to 0.030. Scattering factors were taken from Cromer and Waber.[8] Anomalous dispersion effects[9] were included in F_c; the values for f' and f'' were those of Cromer.[10] In the final cycles of refinement the molybdenum, oxygen, and nitrogen atoms were refined anisotropically. Hydrogen atoms, at their calculated positions were added to the structure factor calculations but their positions were not refined. The structure was refined by using full-matrix least-squares methods. Plots of $\sum(w|F_o| - |F_c|)$ vs. F_o, reflections order in data collection, $(\sin \theta)/\lambda$, and various classes of indices showed no unusual trends. Although $P\bar{4}2_1c$ is a noncentrosymmetric space group, the values of both the investigated and the weighted agreement factors (Table V) were unchanged upon inverting the coordinates of all of the atoms. All calculations were performed on a PDP-11/34a computer using SDP-PLUS.[11]

The final refined atomic coordinates are presented in Table VI, and a selection of the interatomic distances and bond angles is given in Table VII.

Results and Discussion

Nuclear Magnetic Resonance Spectra. The ^{1}H and ^{13}C NMR spectra of [MoO(C$_5$H$_{10}$NO)$_2$(cat)] are shown in Figures 1 and 2, respectively. The relevant details of these spectra are summarized in Tables I and II, together with the corresponding data for the two isomers of the 4-*tert*-butyl-, 4-nitro-, and 3,5-di-*tert*-butylcatechol derivatives. The ^{1}H NMR spectra of these compounds can be divided into two regions, either side of a chemical shift of 5 ppm (downfield of Me$_4$Si). The catechol
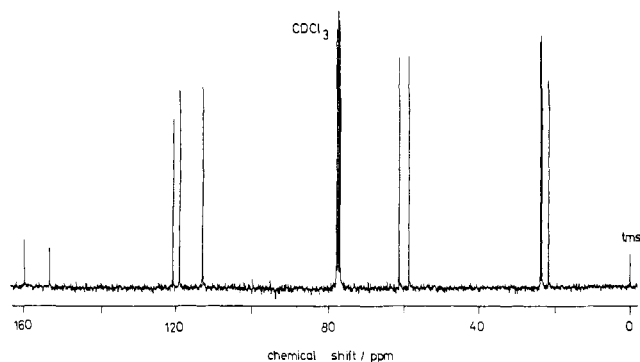
aromatic proton resonances appear as well-resolved singlets, doublets, or triplets in the low-field region; the high-field region comprises the piperidine resonances, which appear as unresolved multiplets, and (where appropriate) intense singlets for the *tert*-butyl groups. Similarly, in the ^{13}C NMR spectra, the resonances of the aromatic catecholate carbons appear significantly downfield of the piperidine and (where appropriate) *tert*-butyl resonances.

The ^{1}H, ^{13}C, and ^{95}Mo (Table III) NMR data obtained are consistent with [MoO(C$_5$H$_{10}$NO)$_2$(cat)] adopting a particular conformation in solution and provide no indication of any inter- or intramolecular rearrangement. Also, the NMR data clearly imply that, apart from the occurrence of isomers, vide infra, the substituted catecholate complexes adopt a structure similar to that of the parent compound. Aspects of this molecular geometry are apparent from specific aspects of the ^{1}H and ^{13}C NMR data. Since four ^{1}H and six ^{13}C resonances of the catecholate ligand are observed, the molecule cannot possess any symmetry element that renders equivalence to atoms of the catecholate ligand, e.g. a C_2 axis. A plane of symmetry containing the catecholate ligand and, of necessity, the oxo group is not excluded. The existence of such a symmetry element is strongly implied by the observation of only eight ^{1}H and five ^{13}C resonances for the piperidine groups of [MoO(C$_5$H$_{10}$NO)$_2$(cat)]. If this plane of symmetry relates half of each piperidine ring to the other half of the *same* ring, then, given the expected[2-5] mode of coordination of 1-piperidinolato(1−),[12] this plane would contain the molybdenum and all the ligand donor atoms, a highly unusual and sterically unfavorable arrangement. However, the alternative postulate, that the two piperidine rings are related by the mirrror plane, does not require any such unlikely geometry. The existence of isomers for the substituted catecholate derivatives (vide infra) indicates that the Mo–O$_t$ axis does not bisect the catecholate moiety; however, the NMR data do not define the relative orientation of the oxo group and the catecholate ligand in the plane of symmetry. Also, the location and orientation of the equivalent 1-piperidinolato(1−) ligands with respect to this plane are not established. These and other details of the molecular structure were obtained, for a crystalline sample of [MoO(C$_5$H$_{10}$NO)$_2$(cat)], by X-ray crystallography.

The detailed assignments of the ^{1}H and ^{13}C NMR spectra involved difficulties. Although the ^{1}H resonances of the aromatic catecholate protons are readily interpreted, especially because of the particular derivatives prepared, the assignments of the corresponding ^{13}C resonances are equivocal. Conversely, the ^{13}C resonances of the piperidine groups are easily elucidated, given the data available for other piperidine derivatives,[13] but this is not the case for their ^{1}H resonances. Therefore, the powerful

(8) Cromer, D. T.; Waber, J. T. "International Tables for X-ray Crystallography"; Kynoch Press: Birmingham, England, 1974; Vol. IV, Table 2.2B.

(9) Ibers, J. A.; Hamilton, W. C. *Acta Crystallogr.* **1964**, *17*, 781.

(10) Cromer, D. T. "International Tables for X-ray Crystallography"; Kynoch Press: Birmingham, England, 1974; Vol. IV, Table 2.3.1.

(11) Frenz, B. A. In "Computing in Crystallography"; Schenk, H., Olthof-Hazelkamp, R., vanKonigsveld, H., and Bassi, G. C., Eds.; Delft University Press: Delft, Holland, 1978; pp 64–71.

(12) The (C$_5$H$_{10}$NO$^-$) fragment has here been named 1-piperidinolate in accordance with IUPAC Recommendations (IUPAC. "Nomenclature of Organic Chemistry Section C, 1979 Edition"; Pergamon Press: Oxford, England, 1979). However, we[5,6] and others[3] have previously termed it piperidine-*N*-oxide or piperidine-*N*-oxo.

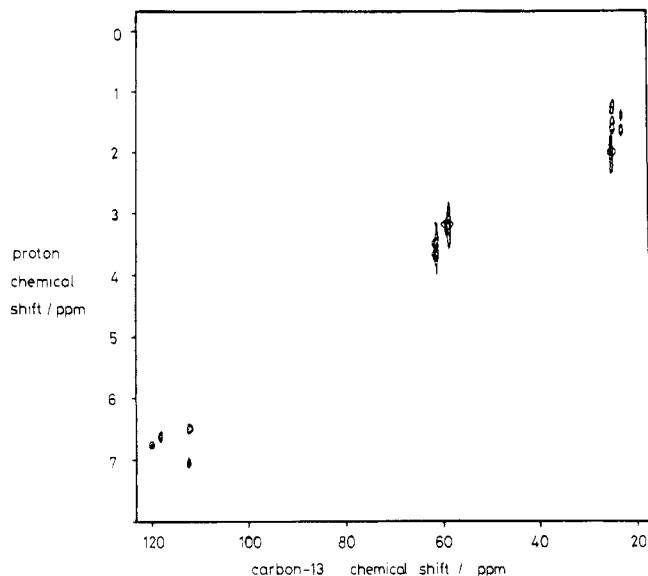(13) Johnson, L. F.; Jankowski, W. C. "Carbon-13 NMR Spectra"; Wiley-Interscience: New York, 1972.

Figure 3. $^{13}C-^1H$ NMR chemical shift correlation for [MoO-$(C_5H_{10}NO)_2(cat)$] in CDCl$_3$. Conditions: ^{13}C 90° pulse = 24 μs, ^1H 90° pulse = 29 μs, 256 transients, 128 increments, spectral widths 8000 × 2500 Hz, Fourier transform size 512 × 512 points, matched sensitivity enhancement in the ^{13}C dimension, total experiment time ca. 14 h.

"two-dimensional" (2D) magnetic resonance techniques, whereby $^1H-^{13}C$ chemical shift correlations and $^1H-^1H$ scalar coupling correlations are identified, were employed to complete the assignments of the ^1H and ^{13}C NMR spectra.

2D-NMR spectroscopy[14-16] greatly increases the amount of information obtainable from NMR. Instead of producing a simple spectrum as a function of frequency $S(f)$, 2D-NMR spectroscopy generates spectra, $S(f_1,f_2)$, as a function of two independent frequencies f_1 and f_2. In the two techniques used in the experiments described below, f_1 and f_2 represent ^1H or ^{13}C chemical shifts. $^1H-^{13}C$ chemical shift correlation[17] produces a spectrum in which one peak appears for each distinct CH group in a molecule. The frequency coordinates, f_1 and f_2, are the ^1H and ^{13}C chemical shift frequencies; by a suitable choice of experimental parameters, the signals seen can be restricted to those from directly bonded CH, CH$_2$, or CH$_3$ groups. The advantages of such spectra are twofold: first, they correlate the ^1H and ^{13}C NMR spectra, identifying those protons and carbons directly bonded to each other, and, second, they allow greatly improved resolving power, since it is very rare for *both* the ^1H and ^{13}C resonances of two CH groups to be accidentally coincident. Although proton–proton multiplet structure can be seen in f_1, under usual experimental conditions the multiplets are unresolved.

Homonuclear correlation,[14,18] the archetype of 2D NMR first proposed by Jeener, identifies scalar couplings between nuclei of the same isotopic species, normally ^1H. Both f_1 and f_2 correspond to the normal proton spectrum; peaks appear with coordinates (δ_A,δ_X) when there is a detectable scalar coupling J_{AX} between protons A and X. Peaks also occur along the diagonal $f_1 = f_2$ with coordinates (δ_A,δ_A) and (δ_X,δ_X). The information obtained from a single 2D experiment is analogous to that which would be found by carrying out a complete set of homonuclear double-resonance experiments. A brief introduction to the use of 2D-NMR experiments is given in ref 19.

2D-NMR spectroscopy proved to be of considerable value in the following respects: (1) The carbon–proton chemical shift correlation (Figure 3) allowed assignment of the ^1H resonances

(14) Aue, W. P.; Bartholdi, E.; Ernst, R. R. *J. Chem. Phys.* **1976**, *64*, 2229.
(15) Freeman, R.; Morris, G. A. *Bull. Magn. Reson.* **1979**, *1*, 5.
(16) Bax, A. "Two-Dimensional NMR Spectroscopy in Liquids"; Reidel: New York, 1982.
(17) Bax, A.; Morris, G. A. *J. Magn. Reson.* **1981**, *42*, 501.
(18) Bax, A.; Freeman, R.; Morris, G. A. *J. Magn. Reson.* **1981**, *42*, 164.
(19) Bhacca, N. S.; Balandrin, M. F.; Kinghorn, A. D.; Frenkiel, T. A.; Freeman, R.; Morris, G. A. *J. Am. Chem. Soc.* **1983**, *105*, 2538.

Figure 4. 300-MHz ^1H NMR spectrum of [MoO(C$_5$H$_{10}$NO)$_2$(3,5-t-Bu$_2$cat)] in CDCl$_3$ (part only).
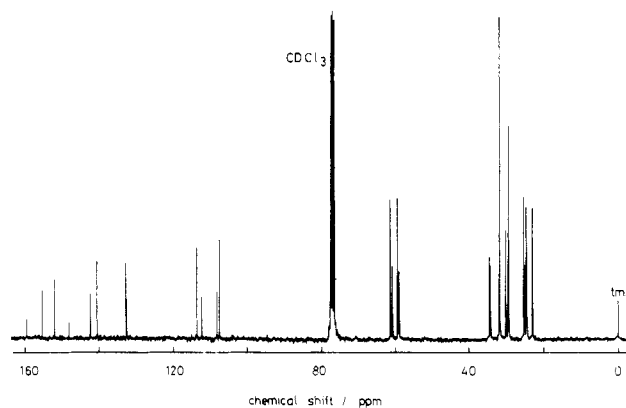
**Figure 5.** 75-MHz ^{13}C NMR spectrum of [MoO(C$_5$H$_{10}$NO)$_2$(3,5-t-Bu$_2$cat)] in CDCl$_3$.

in the piperidine region (Table I) from the ^{13}C assignments (Table II). (The labeling scheme adopted specifies C$_2$ and C$_6$ atoms as α, C$_3$ and C$_5$ atoms as β, and C$_4$ as γ; the attached hydrogen atoms carry the same label.) However, this interpretation remained uncertain, since it was not known whether the ^{13}C resonance labeled β' (Table II) corresponded to a carbon next to α' or whether it was actually due to a carbon (β) next to α. The most straightforward way of removing the ambiguity proved to be by a homonuclear proton coupling correlation. This allowed Table IV to be constructed. The proposed assignments (Table I and II) were confirmed, since H$_\alpha$ was observed to couple to H$_\beta$, H$_{\alpha'}$ to H$_{\beta'}$, and both H$_\beta$ and H$_{\beta'}$ to H$_\gamma$. In addition, and unexpectedly, couplings were also discerned between H$_{\alpha1}$ and H$_{\alpha'}$ and H$_{\alpha2}$ and H$_\gamma$.

(2) The ^{13}C resonances of the catecholate groups of the substituted catecholate complexes were assigned by means of selective proton decoupling experiments. The carbon–proton chemical shift correlation for the unsubstituted catecholate complex (Figure 3) gave the same information in respect of that compound.

(3) The ^1H NMR spectrum of [MoO(C$_5$H$_{10}$NO)$_2$(3,5-t-Bu$_2$-cat)] (Figure 4) contains only three resonances for the

Table I. ¹H NMR Data[a,b] for $[MoO(C_5H_{10}NO)_2(\text{catecholate})]$[c] Complexes

assignt[d]	$[MoO(C_5H_{10}NO)_2(\text{cat})]$	$[MoO(C_5H_{10}NO)_2(4\text{-}t\text{-Bu-cat})]$ isomer		$[MoO(C_5H_{10}NO)_2(3,5\text{-}t\text{-Bu}_2\text{-cat})]$ isomer		$[MoO(C_5H_{10}NO)_2(4\text{-NO}_2\text{-cat})]$ isomer	
		a	b	a	b	a	b
catecholate							
H₃	7.05 ($^3J = 7.8$, $^4J = 1.2$)	7.07 ($^4J = 1.5$)	6.47			7.79 ($^4J = 2.5$)	7.25
H₄	6.73 ($^3J = 7.7$, $^4J = 1.4$)			6.67 ($^4J = 2$)	6.56		
H₅	6.57 ($^3J = 7.6$, $^4J = 1.3$)	6.59 ($^3J = 8.5$, $^4J = 1.5$)	6.74			7.62 ($^3J = 9$, $^4J = 2.5$)	7.78
H₆	6.44 ($^3J = 7.7$, $^4J = 1.4$)	6.35 ($^3J = 8.5$)	6.91	6.36 ($^4J = 2$)	6.97	6.43 ($^3J = 9$)	6.95
tert-butyl							
3				1.50	1.18		
4		1.27	1.19				
5				1.18	1.26		
piperidinolate							
Hα	3.67 / 3.48	3.62 / 3.48		3.66 / 3.40		3.59	
Hα'	3.15	3.14		3.15		3.22 / 3.10	
Hβ	1.98	1.98		1.94[e] / 2.11[e]	2.01[e]	1.99	
Hβ'	1.60 / 1.20	1.61 / 1.28		1.46[e] / 1.13[e]	[f]	1.62 / 1.16	
Hγ	1.67 / 1.40	1.64 / 1.43		1.64[e] / 1.33[e]	1.64[e] / 1.41[e]	1.62 / 1.43	

a Chemical shifts are given in ppm vs. Me₄Si (^nJ/Hz (n = number of bonds through which the coupling occurs)). b Typical conditions for acquiring these spectra: pulse width 8 μs (90° pulse = 8.5 μs); spectral width 3 kHz; 8K data points; 16 transients. c H₂catecholate = 1,2-dihydroxybenzene and its 4-tert-butyl, 3,5-di-tert-butyl, and 4-nitro derivatives. d The labeling of the carbon atoms of the catecholate and piperidine ring are

(catecholate ring labeled: 3, 2, 4, 5, 6, 1, with O, O)

and

(piperidine ring labeled: β', α', γ, N, β, α)
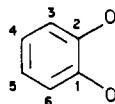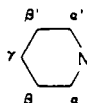
respectively, and the hydrogen atoms or tert-butyl groups are specified according to the carbon atom to which they are bonded. e Obscured by tert-butyl resonances in the one-dimensional spectrum, but shifts obtained from ¹³C-¹H shift correlation. f Intensity too low to be distinguished in the shift correlation.

tert-butyl substituents; these occur at 1.18, 1.26, and 1.50 ppm (and are comparable with the resonances at 1.21 and 1.33 ppm observed for 3,5-di-tert-butylcatechol by Sawyer et al.[20]), thus implying that two of the signals are coincident. However, it is not possible to discern from the integrations which of the peaks contains the two resonances because all three peaks lie on top of the piperidine signals. The ¹³C NMR spectrum of this complex (Figure 5) also contains only three signals attributable to the methyl groups of the tert-butyl moieties. Again, it is not possible to say for certain where the coincidence lies. By means of a proton–carbon chemical shift correlation, however, all four resonances were revealed (Figure 6). Clearly, the proton signal at 1.18 ppm and the ¹³C signal at 31.8 ppm contain the coincident resonances.

The catechol regions of the proton NMR spectra are complicated for the complexes with unsymmetrically substituted catechols, where twice the expected number of resonances are observed. This is ascribed to the presence of geometrical isomers in solution, differing in the relative arrangement of the catecholate ligand with respect to the other ligands. The ratio of the isomers for $[MoO(C_5H_{10}NO)_2(4\text{-NO}_2\text{-cat})]$ and $[MoO(C_5H_{10}NO)_2(4\text{-}t\text{-Bu-cat})]$ is approximately 1:1, that for $[MoO(C_5H_{10}NO)_2(3,5\text{-}t\text{-Bu}_2\text{-cat})]$ is approximately 2:1; these ratios were judged by the relative integrals of respective catecholate proton resonances. The presence of geometrical isomers is confirmed in the (proton-decoupled) ¹³C NMR spectra of the unsymmetrically substituted catechol complexes, with the observation of "extra" resonances at chemical shifts close to those of the unsubstituted catechol complex. Some of the differences in chemical shift between the resonances due to the two isomers are so small as to be unresolved at the highest instrumental frequency routinely available to us (viz. 75 MHz). Figure 7 shows how this isomerism arises. Given that the Mo=O axis does not bisect the catecholate ring, a fixed position for the oxygen atoms leads to two possible orientations of the substituted catecholate with respect to the oxo group. Since the two possible isomers of the 4-substituted catechol adducts are present in roughly equal amounts, substitution in this position clearly does not create any marked steric interaction. However, for $[MoO(C_5H_{10}NO)_2(3,5\text{-}t\text{-Bu}_2\text{-cat})]$ structure IIa is suggested to be the major component, as this would appear to involve less unfavorable steric interactions, between the tert-butyl group on C3 and the piperidine rings of the other ligands, than structure IIb.

The catecholate regions of the ¹³C NMR spectra were assigned, for the protonated carbons, by selective decoupling of the protons and, for the unprotonated carbons, by comparison with the unsubstituted catecholate complex. These latter must, therefore, be regarded as tentative. In the 3,5-di-tert-butylcatechol complex, there is a significant proportion of carbons without attached protons, and consequently, care was needed to obtain a suitable
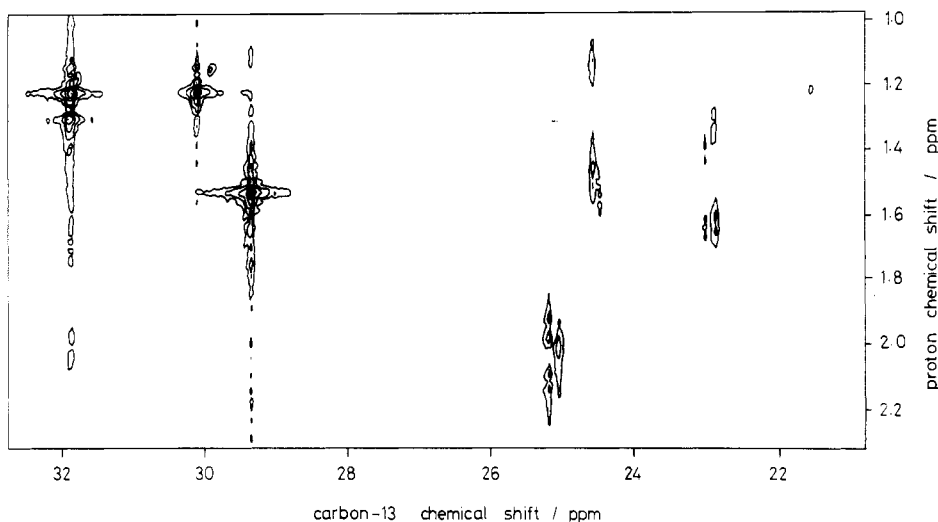
(20) Wilshire, J. P.; Leon, L.; Bosserman, P.; Sawyer, D. T. J. Am. Chem. Soc. **1979**, *101*, 3379.

Figure 6. ^{13}C–^1H NMR chemical shift correlation for [MoO($C_5H_{10}NO$)$_2$(3,5-t-Bu$_2$cat)] in CDCl$_3$. Conditions: ^{13}C 90° pulse = 23 μs, ^1H 90° pulse = 27 μs, 352 transients, 64 increments, spectral widths 900 × 400 Hz, Fourier transform size 512 × 512 points, total experiment time ca. 12 h.

Table II. ^{13}C NMR Data[a,b] for [MoO($C_5H_{10}NO$)$_2$(catecholate)][c] Complexes

assignt[d]	[MoO($C_5H_{10}NO$)$_2$-(cat)]	[MoO($C_5H_{10}NO$)$_2$-(4-t-Bu-cat)] isomer a	b	[MoO($C_5H_{10}NO$)$_2$-(3,5-t-Bu$_2$-cat)] isomer a	b	[MoO($C_5H_{10}NO$)$_2$-(4-NO$_2$-cat)] isomer a	b
catecholate							
1	159.5	157.4[e]	159.4[e]	155.8	160.0	160.0[e]	165.3[e]
2	152.9	152.4[e]	150.2[e]	152.5	148.5	158.4[e]	153.0[e]
3	112.4	110.0	109.6	133.0	132.8	107.5	107.5
4	120.1	143.8[e]	141.9[e]	113.8	112.5	141.0[e]	139.5[e]
5	118.3	114.9	116.7	140.8	142.7	116.1	118.0
6	112.3	111.1	111.2	107.7	108.3	111.3	111.5
***tert*-butyl**							
3 C				34.5[f]			
Me				29.4	30.1		
4 C		34.3[g]	34.0[g]				
Me		31.8					
5 C				34.3[f]			
Me				31.8			
piperidinolate							
α	61.2	61.2[e]	61.0[e]	61.4	60.8	61.8[h]	
α'	58.7	58.8[e]	58.6[e]	59.3	58.9	58.8[h]	
β	25.1	25.2[e]	25.0[e]	25.3	25.1	25.2[h]	
β'	24.8	24.7[h]		24.7	24.5	25.0[h]	
γ	23.0	23.1[h]		23.0	23.1	23.0[h]	

[a] Chemical shifts in ppm vs. Me$_4$Si. [b] Typical conditions for acquiring these spectra: pulse width 18 μs (90° pulse = 23 μs); spectral width 15 kHz; 16K data points; 300 transients; 2–5 s delay between transients; noise decoupler power 3 kHz; 1 Hz line broadening. [c] For specification of ligands see footnote c in Table I. [d] For identification of atoms, see footnote d in Table I. [e] Tentative. Assigned by comparison with the assignments for the isomers of [MoO($C_5H_{10}NO$)$_2$(3,5-t-Bu$_2$-cat)]. [f] May be interchanged. [g] May be interchanged. [h] Resonances due to geometrical isomers not resolved.

Table III. ^{95}Mo NMR Data for [MoO($C_5H_{10}NO$)(catecholate)] Complexes

compd	chem shift[a]/ppm	line width/Hz
[MoO($C_5H_{10}NO$)$_2$(4-NO$_2$-cat)]	−40	450
[MoO($C_5H_{10}NO$)$_2$(cat)]	−5	300
[MoO($C_5H_{10}NO$)$_2$(4-t-Bu-cat)]	17	500
[MoO($C_5H_{10}NO$)$_2$(3,5-t-Bu$_2$-cat)]	−28	400

[a] Relative to 2 M Na$_2$MoO$_4$ in D$_2$O at effective pH 11; ±3 ppm.

Table IV. Homonuclear Proton[a] Scalar Couplings for the Piperidine Groups of [MoO($C_5H_{10}NO$)$_2$(cat)][b]

	H$_{\alpha_1}$	H$_{\alpha_2}$	H$_{\alpha'}$	H$_\beta$	H$_{(\beta'\gamma)}$	H$_\gamma$	H$_{\beta'}$
H$_{\alpha_1}$	×	×	×	×	×		
H$_{\alpha_2}$	×	×		×		×	
H$_{\alpha'}$	×		×		×		×
H$_\beta$	×	×		×	×	×	
H$_{(\beta'\gamma)}$	×		×	×	×	×	×
H$_\gamma$		×		×	×	×	×
H$_{\beta'}$			×		×	×	×

[a] The protons are specified as indicated in the footnotes to Table I. [b] × indicates the presence of a cross-peak in the homonuclear proton coupling correlation.

spectrum because of the long relaxation times. For the 3,5-di-*tert*-butylcatechol complex, the resonances due to the different isomers were distinguished by means of peak intensities. The 4-*tert*-butylcatechol isomers were then differentiated by comparison with these assignments. The *tert*-butyl groups give rise to two types of resonance: that due to the quaternary carbon and that due to the methyl groups. The quaternary carbons give rise to two resonances in each complex; for the 4-*tert*-butylcatechol complex, these are at 34.0 and 34.3 ppm and must be due to the

two isomers. For the 3,5-di-*tert*-butylcatechol complex, they occur at 34.5 and 34.3 ppm and are probably due to the separate *tert*-butyl groups. This conclusion was drawn after examining the ^{13}C NMR spectrum of free 3,5-di-*tert*-butylcatechol, where two resonances are observed.

Table V. Experimental Details of the Crystal Structure
Determination for [MoO(C₅H₁₀NO)₂(cat)]

A. Crystal Data

chem formula	$C_{16}H_{24}MoN_2O_5$
fw	420.32
$F(000)$	1728
cryst color	dark purple
cryst dimens, mm	0.0655 × 0.2070 × 0.3830
peak width at half-height	0.25
Mo Kα radiation	$\gamma = 0.71073$ Å
temp, °C	23 (1)
space group	$P\bar{4}2_1c$
a, Å	14.080 (4)
c, Å	18.099 (8)
V, Å³	3588 (1)
Z	8
ρ_{calcd}, g cm⁻³	1.56
μ, cm⁻¹	7.4

B. Intensity Measurements

instrument	Syntex (Nicolet) P2₁ with modified software
monochromator	graphite crystl, incident beam
cryst–detector dist, cm	21
scan type	θ–2θ
scan rate, deg min⁻¹	1.5–10.0 (in ω)
scan width, deg	1.3 − Kα_1 to Kα_2 + 1.3
max 2θ, deg	50.0
no. of reflcns measd	3592 total, 1791 unique
corrcns	Lorentz–polarization reflcn averaging (agreement on I = 2.9% and on F_o = 2.5%) numerical abs (0.866–0.953; av 0.934)

C. Structure Solution and Refinement

solution	Patterson method
hydrogen atoms	included as fixed contribution to the structure factor
refinement	full matrix least-squares
minimization function	$\sum w(|F_o| - |F_c|)^2$
least-squares wts	$4F_o^2/\sigma^2(F_o^2)$
anomalous dispersion	all non-hydrogen atoms
no. of reflcns included	1080 with $F_o^2 > 3.00\sigma F_o^2$)
no. of params refined	137
unweighted agreement factor	$\sum||F_o| - |F_c||/\sum|F_o| = 0.040$
weighted agreement factor	$(\sum w(|F_o| - |F_c|)^2/\sum wF_o^2)^{1/2} = 0.044$
factor including unobsd data	0.090
esd of observn of unit wt	1.41
convergence, largest shift	0.03
high peak in final difference map, e Å⁻³	1.1

The ¹H and ¹³C NMR spectra for [MoO(C₅H₁₀NO)₂(4-NO₂-cat)] were assigned by selective proton decoupling and by comparison with those of the 4-*tert*-butylcatechol adduct. In general, the spectra are simpler because of the absence of *tert*-butyl groups.

Despite its success in distinguishing between the Λ and Δ isomers of *cis*-[MoO₂((*R*)-cysOMe)₂][21] and *cis*-[MoO₂((*S*)-penOMe)₂],[22] the ⁹⁵Mo NMR spectra of these complexes each showed only one resonance, with unremarkable line widths (see Table III). It is, perhaps, interesting to note that the ⁹⁵Mo nuclei in these complexes are deshielded compared with that in *cis*-[MoO₂(C₅H₁₀NO)₂.].[5,23]

Description of the Structure. The coordination geometry about the molybdenum atom in [MoO(C₅H₁₀NO)₂(cat)] may conveniently be described as distorted pentagonal bipyramidal, with the terminally bound oxo group at one of the apices. This geometry is common for seven-coordinate monooxomolybdenum(VI) complexes.[24] The two 1-piperidinolato(1−) groups are bound side-on

(21) Buchanan, I.; Minelli, M.; Ashby, M. T.; King, T. J.; Enemark, J. H.; Garner, C. D. *Inorg. Chem.* **1984**, *23*, 495.

(22) Buchanan, I.; Garner, C. D.; Clegg, W. *J. Chem. Soc., Dalton Trans.* **1984**, 1333.

(23) Minelli, M.; Enemark, J. H.; Wieghardt, K.; Hahn, M. *Inorg. Chem.* **1983**, *22*, 3952.
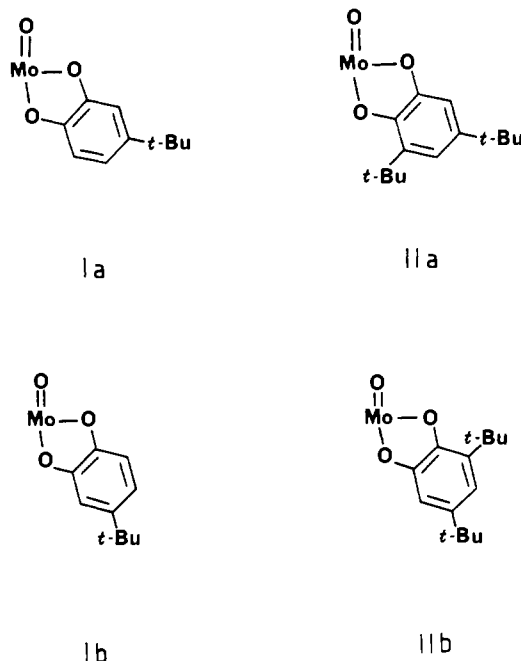
Figure 7. Geometrical isomerism in the *tert*-butylcatecholate complexes.

Table VI. Positional Parameters and Their Estimated Standard Deviations[a]

atom	x	y	z	B_{eq}, Å²
Mo	0.25239 (6)	0.22470 (5)	0.43233 (4)	2.53 (1)
O(1)	0.2543 (6)	0.3438 (5)	0.4220 (4)	4.0 (2)
O(11)	0.1495 (5)	0.2110 (6)	0.5051 (4)	4.2 (2)
O(21)	0.3400 (5)	0.2060 (5)	0.5162 (4)	3.7 (2)
O(31)	0.2513 (5)	0.0839 (4)	0.4136 (3)	2.9 (1)
O(32)	0.2613 (5)	0.2151 (4)	0.3214 (3)	2.9 (1)
N(11)	0.1011 (5)	0.2214 (6)	0.4384 (4)	3.1 (2)
N(21)	0.3992 (5)	0.2176 (6)	0.4558 (5)	3.3 (2)
C(12)	0.0448 (8)	0.3125 (8)	0.4332 (7)	3.9 (2)*
C(13)	0.0052 (9)	0.3216 (8)	0.3579 (6)	4.0 (3)*
C(14)	−0.0527 (8)	0.2376 (9)	0.3353 (6)	4.4 (3)*
C(15)	0.0040 (9)	0.1474 (8)	0.3434 (6)	4.0 (3)*
C(16)	0.0418 (8)	0.1356 (8)	0.4172 (6)	3.8 (3)*
C(22)	0.4567 (8)	0.3034 (8)	0.4596 (6)	3.9 (3)*
C(23)	0.508 (1)	0.3224 (9)	0.3868 (7)	4.8 (3)*
C(24)	0.5675 (8)	0.236 (1)	0.3664 (6)	4.8 (3)*
C(25)	0.5104 (9)	0.1448 (8)	0.3680 (7)	4.2 (3)*
C(26)	0.4603 (8)	0.1341 (8)	0.4409 (7)	3.8 (2)*
C(31)	0.2532 (8)	0.0519 (6)	0.3432 (5)	2.8 (2)*
C(32)	0.2510 (8)	−0.0418 (6)	0.3188 (5)	2.9 (2)*
C(33)	0.250 (1)	−0.0589 (7)	0.2442 (7)	4.4 (2)*
C(34)	0.2568 (9)	0.0144 (7)	0.1929 (5)	4.0 (2)*
C(35)	0.2608 (8)	0.1077 (7)	0.2161 (5)	3.1 (2)*
C(36)	0.2594 (8)	0.1259 (6)	0.2905 (5)	2.6 (2)*

[a] Starred values indicate atoms were refined isotropically. Anisotropically refined atoms are given in the form of the isotropic equivalent thermal parameter defined as $8\pi^2(U_{11} + U_{22} + U_{33})/3$.

Table VII. Selected Bond Lengths (Å) and Interbond Angles (deg) for [MoO(C₅H₁₀NO)₂(cat)][a]

Mo–O(1)	1.688 (6)	O(1)–Mo–O(11)	100.6 (4)
Mo–O(11)	1.967 (7)	O(1)–Mo–O(21)	102.0 (3)
Mo–O(21)	1.975 (7)	O(1)–Mo–O(31)	163.9 (3)
Mo–O(31)	2.012 (5)	O(1)–Mo–O(32)	87.4 (3)
Mo–O(32)	2.016 (5)	O(1)–Mo–N(11)	92.5 (4)
Mo–N(11)	2.134 (8)	O(1)–Mo–N(21)	93.1 (4)
Mo–N(21)	2.112 (8)	O(11)–Mo–N(11)	39.5 (3)
N(11)–O(11)	1.393 (10)	O(21)–Mo–N(21)	39.4 (3)
N(21)–O(21)	1.385 (10)	O(31)–Mo–O(32)	76.5 (2)
C(31)–O(31)	1.352 (9)	N(21)–Mo–O(32)	97.8 (3)
C(36)–O(32)	1.375 (9)	N(11)–Mo–O(32)	96.4 (3)
C(31)–C(36)	1.415 (11)	O(21)–Mo–O(11)	86.1 (3)

[a] Numbers in parentheses are estimated standard deviations in the least significant digits.

Table VIII. Cyclic Voltammetric[a] Data Obtained[b] for [MoO($C_5H_{10}NO)_2$(catecholate)] Complexes

compd	reduction				oxidation			
	E_p/V	$E_{p/2}$V	Δ	rev	E_p/V, E/V	$E_{p/2}$/V	Δ	rev
[MoO($C_5H_{10}NO)_2$(4-NO_2-cat)]	−1.43 reox at 0.43	−1.29	0.14	×	1.07	0.98	0.09	×
[MoO($C_5H_{10}NO)_2$(cat)]	−1.71 reox. at 0.01	−1.53	0.18	×	0.66	0.58	0.08	×
[MoO($C_5H_{10}NO)_2$(4-t-Bu-cat)]	−1.83 reox at 0.0	−1.55	0.28	×	0.53			√
[MoO($C_5H_{10}NO)_2$(3,5-t-Bu_2-cat)]	−1.92 reox at −0.02	−1.66	0.26	×	0.47			√

[a] Key: E_p, peak potential; $E_{p/2}$, half-peak potential; E, reversible redox potential; Δ, shape factor ($=E_{p/2} - E_p$) at scan rate of 0.3 V s^{-1}; ×, not reversible; √, reversible. [b] See ref 7 for specification of experimental details.
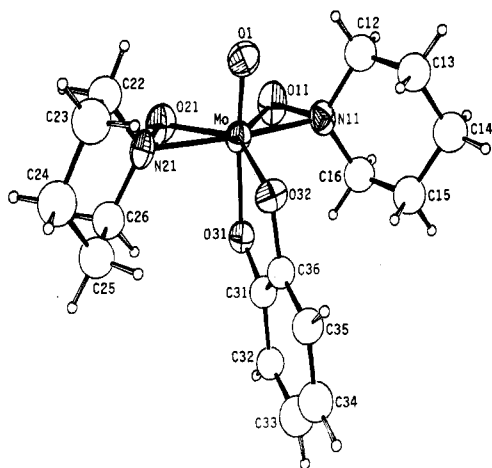
Figure 8. ORTEP plot of the molecular structure of [MoO($C_5H_{10}NO)_2$-(cat)]. Thermal ellipsoids are plotted at the 50% probability level.

as expected,[3-6,25-30] and occupy four of the equatorial positions. The catecholate(2−) ligand spans an equatorial and an apical position. The molecular structure of [MoO($C_5H_{10}NO)_2$(cat)] is depicted in Figure 8, and selected bond lengths and interbond angles are given in Table VII. As predicted from the NMR data, the molecular structure closely corresponds to C_s point symmetry, with the catecholate coordinated asymmetrically with respect to the Mo–O_t axis.

A comparison between the structure of this compound and its parent,[3] *cis*-[MoO_2($C_5H_{10}NO)_2$], reveals three significant changes induced by coordination of the catecholate ligand, namely (i) shortening of the Mo–O_t bond from an average value[3] of 1.79 Å to 1.69 Å, the latter being typical of Mo–O bonds of order 2.5,[31] (ii) movement of the remaining oxo ligand toward the oxygen atoms of the 1-piperidinolato(1−) groups by 14.8°, and (iii) shortening of the N–O bond in the 1-piperidinolato(1−) ligands from 1.434 (10) and 1.465 (10) Å to 1.385 (10) and 1.394 (10) Å. This may be indicative of increased π-donation to the metal by the 1-piperidinolato(1−) group, following replacement of one strongly π-donating oxo group by catecholate. Apart from this decrease in N–O bond length, the dimensions of the 1-piperidinolato(1−) ligands and their overall geometry about molybdenum are essentially the same in the two complexes.

One possible description of the coordination geometry of [MoO($C_5H_{10}NO)_2$(cat)] is that of a distorted trigonal bipyramid,

involving a trigonal plane containing O(32) and the centroids of the two N–O groups; the relevant interbond angles in the trigonal plane would then be ca. 110, 116, and 126°. However, we prefer to regard both N and O atoms of the 1-piperidinolato(1−) ligand as donors and, therefore, favor a distorted pentagonal-bipyramidal description of the coordination geometry. The interbond angles between the atoms in the equatorial plane of the pentagonal bipyramid are irregular because of the short N–O distances (see Table VII). Also, the angle subtended by the apical atoms at the molybdenum, O(1)–Mo–O(31), is only 163.9 (3)°. This latter distortion is typical[32] of monooxomolybdenum complexes, in which a chelating ligand occupies two sites—one trans and one cis to the terminal oxo group—and often appears to arise because the angle between the oxo group and the chelate donor atom cis to the oxo group is *acute*. Such a geometry is remarkble because, in general, the molybdenum atom is displaced from the plane of the equatorial ligands toward the apical oxo group. This condition is observed in [MoO($C_5H_{10}NO)_2$(cat)], with O(1)–Mo–O(32) = 87.4(3)°, even though the molybdenum is displaced 0.14 Å from the pentagonal plane toward O(1). The irregular stereochemistries found for oxomolybdenum(VI) complexes have been rationalized in terms of repulsive nonbonded interactions between the oxo group and the donor atoms of the chelate ligands;[33,34] such effects are considered to be important for [MoO($C_5H_{10}NO)_2$(cat)].

The structure of several seven-coordinate oxomolybdenum(VI) complexes containing η²-alkylhydroxylamido(1−) ligands have been determined.[25-29] However, [MoO($C_5H_{10}NO)_2$(cat)] is the first such structure with a symmetrical chelating ligand spanning an equatorial and an axial position of a distorted pentagonal bipyramid. As such, this compound provides a unique opportunity to compare directly Mo–O_{cat} distances that are cis and trans to the terminal oxo group. The cis (Mo–O(32) = 2.016 (5) Å) and trans (Mo–O(31) = 2.012 (5) Å) distances are indistinguishable. As a comparison, the nonbridging Mo–O_{cat} distances in [Mo_2O_5(3,5-t-Bu_2-cat)$_2$]$^{2-}$ are 1.98(1)Å.[36] The equivalent cis and trans Mo–O_{cat} distances in [MoO($C_5H_{10}NO)_2$(cat)] contrast sharply with the results recently reported[37] for [MoO($O_2)_2$(bpy)], where the 2,2′-bipyridyl ligand spans an equatorial and an axial position of a distorted pentagonal bipyramid. This compound exhibits a strong static trans effect, with Mo–N_{eq} = 2.199 (5) Å and Mo–N_{ax} = 2.312 (5) Å. Although not unprecedented for monooxomolybdenum(VI) complexes,[26] the absence of a static trans effect in [MoO($C_5H_{10}NO)_2$(cat)] is remarkable.

The lengths of the C–O bonds, C(36)–O(32) = 1.376 (9) Å and C(31)–O(31) = 1.352 (9) Å, are typical of values observed in other catecholate(2−) complexes[38] and in free catechol itself.[39]

Electrochemical Studies. The electrochemical behavior of [MoO($C_5H_{10}NO)_2$(cat)] and its 4-nitro-, 4-*tert*-butyl-, and 3,5-di-*tert*-butylcatecholate derivatives, in MeCN solution, has been

(24) See, for example: Stomberg, R. *Acta. Chem. Scand.* **1970**, *24*, 2024. Le Carpentier, J. M.; Schlupp, R.; Weiss, R. *Acta Crystallogr., Sect. B: Struct. Crystallogr. Cryst. Chem.* **1972**, *B28*, 1278. Dirand, J.; Ricard, L.; Weiss, R. *J. Chem. Soc., Dalton Trans.* **1976**, 278. Reference 37.
(25) Holzbach, W.; Wieghardt, K.; Weiss, J. *Z. Naturforsch., B: Anorg. Chem., Org. Chem.* **1981**, *36B*, 298.
(26) Wieghardt, K.; Holzbach, W.; Hofer, E.; Weiss, J. *Chem. Ber.* **1981**, *114*, 2700.
(27) Wieghardt, K.; Hofer, E.; Holzbach, W.; Nuber, B.; Weiss, J. *Inorg. Chem.* **1980**, *19*, 2927.
(28) Liebeskind, L. S.; Sharpless, K. B.; Wilson, R. D.; Ibers, J. A. *J. Am. Chem. Soc.* **1978**, *100*, 7061.
(29) Wieghardt, K.; Holzbach, W.; Hofer, E.; Weiss, J. *Inorg. Chem.* **1981**, *20*, 343.
(30) Wieghardt, K.; Holzbach, W.; Weiss, J. *Inorg. Chem.* **1981**, *20*, 3436.
(31) Cotton, F. A.; Wing, R. M. *Inorg Chem.* **1965**, *4*, 867.

(32) Yamanouchi, K.; Huneke, J. T.; Enemark, J. H.; Taylor, R. D.; Spence, J. T. *Acta Crystallogr., Sect. B: Struct. Crystallogr. Cryst. Chem.* **1979**, *B35*, 2326 and references therein.
(33) Kepert, D. L. *Prog. Inorg. Chem.* **1977**, *23*, 1.
(34) Yamanouchi, K.; Enemark, J. H. *Inorg. Chem.* **1979**, *18*, 1926.
(35) Stiefel, E. I. *Prog. Inorg. Chem.* **1977**, *22*, 1 and references therein.
(36) Pierpont, C. G.; Buchanan, R. M. *Inorg. Chem.* **1982**, *21*, 652.
(37) Schlemper, E. O.; Schrauzer, G. N.; Hughes, L. A. *Polyhedron* **1984**, *3*, 377.
(38) Pierpont, C. G.; Buchanan, R. M. *Coord. Chem. Rev.* **1981**, *38*, 45 and references therein.
(39) Brown, C. J. *Acta Crystallogr.* **1966**, *21*, 170.

Table IX. IR and UV–Vis Spectroscopic Data for the Complexes

compd	IR ν(Mo–O)/ cm^{-1}	UV–vis^a/nm
[MoO(C₅H₁₀NO)₂(4-NO₂-cat)]	925	470 (5700), 372 (6800), 307 (6900), 225 (12 250)^b
[MoO(C₅H₁₀NO)₂(cat)]	921	512 (3900)
[MoO(C₅H₁₀NO)₂(4-t-Bu-cat)]	919	534 (4800)
[MoO(C₅H₁₀NO)₂(3,5-t-Bu₂-cat)]	920	550 (4900)

^{a} Extinction coefficient in parentheses in dm³ mol^{-1} cm^{-1}. ^{b} Only the 4-nitrocatecholate compound showed distinct peaks below ca. 500 nm.

investigated by variable scan rate cyclic voltammetry and controlled-potential electrolysis. Trends within the electrochemical data obtained for this homologous series of complexes were of interest, as was a comparison with the electrochemical properties of cis-[MoO₂(C₅H₁₀NO)₂].[7]

Each of these catecholate complexes undergoes an irreversible reduction, at a Pt-wire electrode in the vicinity of −1.5 V vs. the [Fe(η⁵-C₅H₅)₂]⁺/[Fe(η⁵-C₅H₅)₂] couple, to yield a product which is reoxidized on the reverse scan at ca. 0 V. We were unable to observe a reversible reduction process, even at fast scan rates and low temperatures (ca. 230 K). Clearly, the substitution of an oxo group by a catecholate ligand causes a marked decrease in the peak reduction potential, from −2.50 V for cis-[MoO₂-(C₅H₁₀NO)₂][7] to −1.71 V for [MoO(C₅H₁₀NO)₂(cat)], as expected in view of the rich electrochemistry identified for molybdenum–catecholate complexes.[40,41] Furthermore, as shown in Table VIII, the values of the half-peak ($E_{p/2}$) and peak (E_p) reduction potentials vary in the expected manner as the substituents on the catecholate(2−) ligand are varied; viz., reduction becomes less thermodynamically facile as electron-donating groups are added to the catecholate ring and more facile for the electron-withdrawing nitro group.

The peak reduction current, i_p^{red}, for each of these catecholate complexes is approximately half of that for a reversible one-electron process, while the shape factor, $E_p^{red} - E_{p/2}^{red}$, is ca. 150–300 mV: both observations are indicative of sluggish, one-electron-transfer kinetics. The peak current function $i_p^{red}/v^{1/2}$ varies with scan rate v, deviating at slow scan rates toward a nominal two-electron reduction process. Controlled-potential electrolysis of [MoO(C₅H₁₀NO)₂(cat)] in acetonitrile at a mercury surface confirms that, on the preparative time scale, two electrons per molecule are consumed to produce a yellow, diamagnetic solution. The product of this reduction has not been identified.

Each of the catecholate complexes undergoes a one-electron oxidation process. This is undoubtedly based on the catecholate ligand, given the failure to detect an electrochemical oxidation for cis-[MoO₂(C₅H₁₀NO)₂].[7] The stability of the radical cation generated depends on the nature of the substituted catecholate. Whereas the unsubstituted- and 4-nitrocatecholate complexes oxidize essentially irreversibly even at fast scan rates, the tert-butyl-substituted species undergo a primary one-electron transfer, which is reversible at scan rates ⩾0.1 V s^{-1}. The stability of the tert-butyl-substituted radical cations may be a consequence of the tert-butyl groups +I inductive effect stabilizing the cation charge, and/or their steric bulk: both of these properties would inhibit attack on the cation by a solution nucleophile. Variable scan rate cyclic voltammetry clearly showed that the oxidation, reversible or not, deviates toward a two-electron process at scan rates <0.3 V s^{-1}. As noted for the reduction potentials, the half-peak or reversible oxidation potentials (Table VIII) vary as expected with substitution of the catecholate ring, oxidation becoming thermodynamically more facile as electron-donating groups are added

to the ring and less facile for the electron-withdrawing nitro group.

IR, UV–Vis, and Mass Spectroscopic Data. A sharp, relatively intense band appears at ca. 920 cm^{-1} in the IR spectrum of [MoO(C₅H₁₀NO)₂(cat)] and its substituted derivatives (Table IX). This band is assigned to ν(Mo–O$_t$) by comparison with the IR spectra of the respective free ligands and of cis-[MoO₂-(C₅H₁₀NO)₂].[5] Two bands between 950 and 1000 cm^{-1} are present in the IR spectrum of each complex; however, these are considered to be 1-piperidinolate ligand vibrations. In comparison with the ν(Mo–O$_t$) stretching frequencies of other monooxomolybdenum complexes[27,29,35,42] the value for these complexes seems slightly low, even though the Mo–O$_t$ bond length is normal.

The visible spectrum of each of these complexes is dominated by an absorption at ca. 500 nm ($\epsilon \sim 5000$ dm³ mol^{-1} cm^{-1}) (Table IX). This is considered to be a catecholate-to-metal charge-transfer transition and, as would be expected, moves to lower energy with an increase in the electron-donating ability of the substituents on the catecholate moiety.

Each of the complexes prepared in this study may be readily sublimed in vacuo, and each yields a mass spectrum with a comparatively weak, but definite, parent molecular ion.

Conclusions

cis-[MoO₂(C₅H₁₀NO)₂] reacts with catechols, replacing one oxo group by a catecholate(2−) ligand, to form a discrete molecular complex of composition [MoO(C₅H₁₀NO)₂(catecholate)]. The preference for loss of an oxo group rather than a 1-piperidinolato(1−) ligand is a clear testimony of the kinetic and/or thermodynamic stability of the ligation to molybdenum achieved by these N,O-chelates.

We have demonstrated that the techniques of 2D-NMR spectroscopy, already applied widely in organic chemistry, are eminently applicable in coordination chemistry. The resultant simplification of the assignment of complicated NMR spectra, particularly where resonances overlap, permits more definitive structural conclusions to be reached.

[MoO(C₅H₁₀NO)₂(cat)] is another example of a monooxomolybdenum(VI) complex with a distorted pentagonal-bipyramidal geometry. However, this complex is rare in exhibiting no lengthening of the bond trans to the oxo group.

Each of these complexes is capable of electrochemical oxidation and reduction; the one-electron oxidation is reversible under certain conditions for the complexes containing the 4-*tert*- and 3,5-di-*tert*-butylcatecholate(2−) ligands.

(40) Charney, L. M.; Schultz, F. A. *Inorg. Chem.* **1980**, *19*, 1527.

(41) Charney, L. M.; Finklea, H. O.; Schultz, F. A. *Inorg. Chem.* **1982**, *21*, 549.

(42) Buchanan, R. M.; Pierpont, C. G. *Inorg. Chem.* **1979**, *18*, 1616.